Direct Detection of High Mobility around Chain Ends of Poly(methyl methacrylate) by the Spin-Labeling

Yohei Miwa,[†] Katsuhiro Yamamoto,[†] Masato Sakaguchi,[‡] Masahiro Sakai,[§] Seiji Makita,[§] and Shigetaka Shimada*,[†]

Department of Materials Science & Engineering, Nagoya Institute of Technology, Gokiso-cho, Showa-ku, Nagoya 466-8555, Japan; Nagoya Keizai University, 61 Uchikubo, Inuyama, 484-8503, Japan; and Research Center for Molecular-Scale Nanoscience, Institute for Molecular Science, 38 Nishigo-Naka, Myodaiji, Okazaki 444-8585, Japan

Received August 19, 2004; Revised Manuscript Received November 28, 2004

ABSTRACT: Effects of chain ends on the dynamics of atactic poly(methyl methacrylate) (PMMA) was studied by the spin-label technique. PMMA's with well-defined molecular weights were synthesized by atom transfer radical polymerization and selectively labeled at the end or inside sites of the chain with a stable nitroxide radical. The WLF treatment demonstrated that a transition temperature, $T_{5.0mT}$, at which an extreme separation width was 5.0 mT, reflected the glass transition observed at a frequency of electron spin resonance (ESR). The $T_{5.0mT}$ of the PMMA labeled at the chain end ($T_{5.0mT,e}$) was ca. 8 K lower than that of the PMMA labeled at the inside sites ($T_{5.0mT,i}$). From the comparison of some polymers, the difference between the $T_{5.0mT,i}$ and $T_{5.0mT,e}$ of a rigid polymer was found to be larger than that of a flexible polymer. The $T_{5.0mT,i}$ and $T_{5.0mT,e}$ decreased with a decrease in the molecular weight as well as a glass transition temperature determined by calorimetric measurements. This result supports that the $T_{5.0mT}$ reflects the glass transition of the PMMA and suggests that the cooperative motion with neighboring segments is necessary for not only inside segments but also chain ends to undergo a rotational relaxation. The high mobility around chain ends brought a shorter correlation time (τ_c) at the region around chain ends. Moreover, a model on the basis of an arrangement of segments suggested that an encounter of chain ends was unable to be ignored in the case of low molecular weights, and the encounter of chain ends locally induced a much shorter τ_c around them.

Introduction

Chain ends play important and interesting roles on a glass transition of polymers. Considering a polymer as a copolymer comprised of inside units and mobile end groups, Ueberreiter and Kanig derived the relationship between a glass transition temperature (T_g) and a number-averaged molecular weight (M_n).[1]

$$1/T_g = 1/T_{g\infty} + A/M_n \quad (1)$$

Here, $T_{g\infty}$ is a value of the T_g at an infinite molecular weight and A is a constant. In fact, we detected higher mobility around chain ends than that of inside segments of polystyrene (PS), poly(methyl acrylate) (PMA), poly(cyclohexyl acrylate) (PCHA), and poly(cyclohexyl methacrylate) (PCHMA) by the spin-label technique.[2−4] Computer simulation works also supported the higher mobility around chain ends in the bulk.[5,6] The higher mobility around chain ends can be rationalized in the free volume model, the entropy model, and the coupling model by the chain ends having respectively excess free volume, excess configurational entropy, and deficient intermolecular constraints.[7,8]

Sung et al. detected larger specific free volume around chain ends than that around inside segments of PS by the photolabel method.[9,10] Li et al. detected the relatively large specific free volume around PS chain ends by the positron annihilation lifetime technique and suggested the high mobility of the chain ends.[11] Richardson et al. reported that each PS chain end had larger local free volume than the average local free volume per repeat unit by dilatometric measurements.[12] These results suggest that the high mobility and large free volume around the chain end correlate with each other. In fact, Kanaya et al. demonstrated that the molecular mobility of *cis*-1,4-poly(butadiene) was bound up with the free volume size.[13,14]

Chain ends often affect the dynamics of polymeric materials remarkably. Angell introduced the concept of "fragility" to understand the mechanism of the glass formation.[15] According to his concept, the "strength" or "fragility" of relaxation behavior reflects the topology of the potential energy hypersurface governing diffusions, reorientations, and, for the case of polymers, segmental reconfigurations.[16−18] Santangelo et al. estimated the molecular weight dependence of the "fragility" of PS,[19] and a decrease in the fragility of the PS with a reduction of the molecular weight was indicated. Santangelo et al. interpreted that this behavior was brought from an increase in any configurational freedom conferred by chain ends. Rizos and Ngai reported that the distribution of the relaxation time of a low molecular weight PS (M_n = 1100) was strongly temperature-dependent and narrowed with increasing temperature, in contrast with a high molecular weight PS.[20] By considering the low molecular weight polymer as a blend of chain ends and inside repeat units, the results were interpreted by the coupling model. This result obviously indicates that the mobility around chain ends is different from that of inside segments, and effects of chain ends on overall dynamics are unable to be ignored when the concentration of chain ends is high. Recently, Casalini et al. reported an interesting behavior relative

[†] Nagoya Institute of Technology.
[‡] Nagoya Keizai University.
[§] Institute for Molecular Science.
* Corresponding author: e-mail shimada.shigetaka@nitech.ac.jp.

10.1021/ma048287y CCC: $30.25
Published on Web 01/14/2005

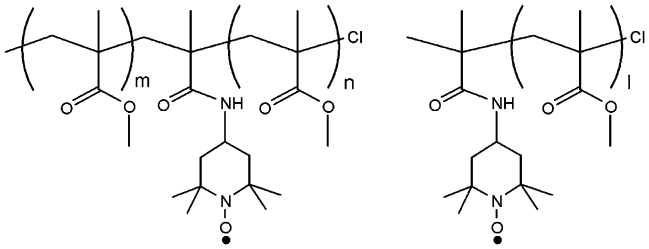

Figure 1. Chemical structures of PMMA spin-labeled at inside (left) and end (right) of chain.

to chain ends. They carried out dynamic mechanical and dielectric spectroscopy measurements on a polychlorinated biphenyl (PCB54), an oligomeric PS (PS590), and their blend,[21] and they found that the addition of the PS590 speeded up dielectric relaxation of the PCB54, even though the former had a higher T_g. They concluded that excess chain ends of PS590 might play important roles in this behavior, but it is still uncertain.

The cooperative volume relevant to the chain dynamics is still one of the unclear problems. Inoue and Osaki showed via a combination of rheological and rheooptical measurements that the "rubbery" relaxation spectrum terminates with a fastest Rouse mode that, for many polymers, corresponds well to the Kuhn length (l_k).[22] Recently, Lodge and McLeish estimated that the cooperative volume at the glass transition was comparable to the l_k^3 for miscible polymer blends.[23] Some experimental results bolstered their idea.[24−26] Moreover, Haley et al. reported that the cooperative volume relevant to the dynamics of the components in the blend was nearly temperature-independent above the T_g.[27] Recently, segmental dynamics of PCHMA and PCHA in their miscible blend was estimated by the spin-label technique, and the volume to influence the motion of spin-labels was suggested to be comparable to the l_k^3.[28]

In the present work, the dynamic features of chain ends of the PMMA were focused on. The high mobility around chain ends was directly detected by the spin-label technique. Moreover, the molecular weight dependence of the mobility around chain ends, the cooperativity between chain ends and inside segments, and the size of the cooperative motion were discussed.

Experimental Section

Materials. Inhibitors in methyl methacrylate (MMA, Extra Pure Reagent, Nacalai Tesque Co., Ltd.) and *tert*-butyl methacrylate (*t*BMA, Extra Pure Reagent, Tokyo Chemical Co., Ltd.) were adsorbed to activate aluminum oxide (particle size 2−4 mm, Kanto Chemical Co., Inc.) and removed. 1,1,4,7,10,10-Hexamethyltriethylenetetramine (HMTETA, 97%, Aldrich Chemical Co., Ltd.), methyl α-bromoisobutyrate (MBIB, 99%, Fluka Chemical Co., Ltd.), *tert*-butyl α-bromoisobutyrate (*t*BBIB, 99%, Fluka Chemical), CuCl (95%, Nacalai Tesque), ethylenediaminetetraacetic acid (EDTA, Guaranteed Reagent, Nacalai Tesque), NaOH (Guaranteed Reagent, Nacalai Tesque), distilled water (Specially Prepared Reagent, Nacalai Tesque), dithranol (97%, Aldrich), and 2,2,6,6-tetramethyl-4-aminopiperidine-1-oxyl (4-amino-TEMPO, 99%, Aldrich) were used as received. Tetrahydrofuran (THF), toluene, anisole, acetone, and methanol (Extra Pure Reagent) were obtained from Nacalai Tesque and used without further purification.

Sample Preparation and Selective Spin-Label. 1. Chain End of PMMA (Figure 1, Right). Atactic PMMA's used in this study were synthesized by atom transfer radical polymerization (ATRP) with the CuCl/HMTETA complex and *t*BBIB as an initiator in anisole at 363 K.[29,30] The polymerization was carried out in vacuum conditions. As a result, PMMA which had a *tert*-butyl moiety at the α end was prepared. The reaction mixture was dissolved into toluene and washed with water solution of EDTA/2Na (2 wt %) to remove the copper. For spin-labeling, an amide−ester interchange reaction between the *tert*-butyl moiety at the chain end and 4-amino-TEMPO was carried out in toluene at 283 K for 4 days. The PMMA was precipitated from acetone solution to water/methanol mixture, filtered to remove the large amount of unreacted spin-label reagents, and finally dried in a vacuum at 393 K for 24 h. This precipitation was repeated more than four times to completely remove the unreacted spin-label reagents. In the case of small molecular weight (M_n) samples, the labeling concentration becomes relatively too high. Therefore, the unlabeled PMMA with the identical M_n, which was initiated with MBIB, was blended to dilute the concentration in order to avoid the influence of the spin-labels on the overall T_g (molecular dynamics).

2. Inside of PMMA Chain (Figure 1, Left). Poly(MMA-*random*-*t*BMA) was prepared by random copolymerization of MMA and *t*BMA using the ATRP technique.[31] The initial molar composition of MMA:*t*BMA = 99:1 and MBIB was used as an initiator. The other conditions of the polymerization were the same with that mentioned above. The *tert*-butyl moieties in the poly(MMA-*random*-*t*BMA) were reacted with 4-amino-TEMPO. The sample was purified by the same procedure in the case of the end-labeled PMMA.

The number-averaged molecular weight (M_n) and its distribution (M_w/M_n) of the spin-labeled PMMA's were determined by gel permeation chromatography (GPC) using PMMA standards (Polymer Laboratories, Ltd.) The PMMA's had a small M_w/M_n ranging from 1.05 to 1.30. The M_n's of low molecular weight PMMA's were determined by matrix-assisted laser desorption ionization, time-of-flight mass spectrometry (MALDI-TOF-MS).[32,33]

Measurement. GPC was carried out with following conditions: in THF (1 mL/min) at 313 K on four polystyrene gel columns (Tosoh TSK gel GMH (beads size is 7 μm), G4000H, G2000H, and G1000H (5 μm)) that were connected to a Tosoh CCPE (Tosoh) pump and an ERC-7522 RI refractive index detector (ERMA Inc.). The columns were calibrated against standard PMMA (Polymer Laboratories, Ltd.) samples.

Each sample was contained in a quartz tube, and the tube was depressurized to a pressure of 10^{-4} Torr and sealed before ESR measurement. ESR spectra at 77 K and higher temperatures were observed at low microwave power level to avoid power saturation and with 100 kHz fielded modulation using JEOL JES-FE3XG and JES-RE1XG spectrometers (X band) coupled to microcomputers (NEC PC-9801). The signal of 1,1-diphenyl-2-picrylhydrazyl (DPPH) was used as a *g* tensor standard. The magnetic field was calibrated with the well-known splitting constants of Mn^{2+}.

Differential scanning calorimetry (DSC, MDSC 2920) manufactured by TA Instruments was used. Samples were heated from a room temperature to 453 K with a rate of 20 K/min, kept for 5 min, and cooled with a rate of 10 K/min. The data collection was carried out on the cooling process. The calorimeter was calibrated with an indium standard.

The MALDI-TOF-MS spectra (in linear mode) were obtained using a PreSeptive Biosystems Voyager DE-STR instrument, equipped with a N_2 laser at 337 nm to determine the M_n of the PMMA. Dithranol, 0.1 M in THF, doped with Na^+, was used as the matrix solution.

Results and Discussion

1. High Molecular Mobility around Chain Ends. Temperature-dependent ESR spectra of the PMMA's labeled at the end and the inside of the chain are compared from 77 to 450 K (Figure 2). The M_n's of the both spin-labeled PMMA's are 9.2K. The temperature dependence of the spectra is brought from the change of the τ_c of the spin-labels. The outermost splitting width of main triplet spectrum induced by hyperfine coupling caused by the nitrogen nucleus narrows with an increase in mobility of the radicals because of motional

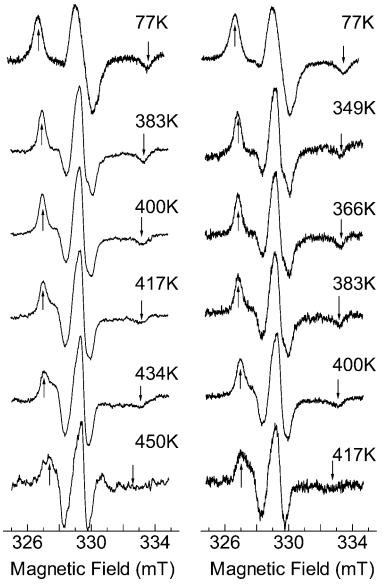

Figure 2. Comparison of temperature-dependent ESR spectra of PMMA labeled at inside (left, M_n = 9.2K, M_w/M_n = 1.21) and end (right, M_n = 9.2K, M_w/M_n = 1.22) of chain. Separation between arrows shows extreme separation width.

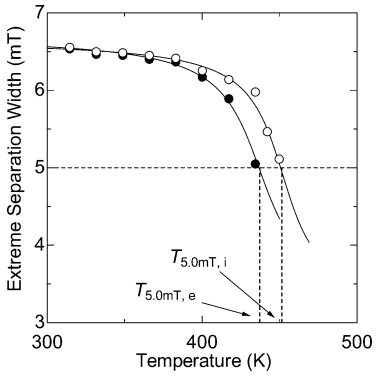

Figure 3. Temperature-dependent extreme separation width of ESR spectra of PMMA labeled at inside (open) and end (solid) of chain shown in Figure 2.

averaging of the anisotropic interaction between an electron and a nucleus. The complete averaging gives rise to an isotropic narrowed spectrum.[28] However, the isotropic narrowed spectrum was not observed for these samples in this temperature range because of a high viscosity of the PMMA. A temperature dependence of the extreme separation width between arrows in Figure 2 is shown in Figure 3. The extreme separation width gradually decreases and steeply drops with an increase in temperature. This steep drop is caused by a micro-Brownian-type molecular motion.[2,34−36] The gradual decreasing of the extreme separation width in the low-temperature range (below the steep drop of the extreme separation width) is induced by local motion of the spin-labels in structural defects.[37]

$T_{5.0mT}$, at which the extreme separation width is equal to 5.0 mT, is estimated as a transition temperature of the molecular motion. The $T_{5.0mT}$'s of the PMMA labeled at the inside ($T_{5.0mT,i}$) and the chain end ($T_{5.0mT,e}$) are 452 and 437 K, respectively. In this work, the $T_{5.0mT}$'s included somewhat large experimental uncertainties of ±4 K because of noisy spectra from the low spin-label concentration and the thermal degradation of the spin-labels at higher temperatures. Moreover, it was unable to measure more than 450 K because of the considerable

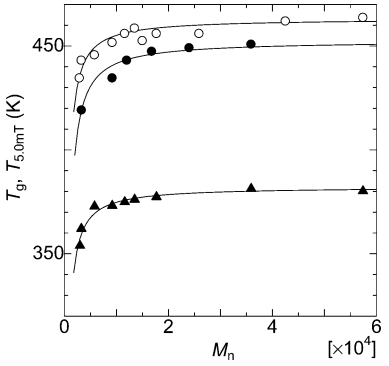

Figure 4. Plots of $T_{5.0mT,i}$ (open) and $T_{5.0mT,e}$ (solid) and $T_{g,DSC}$ (triangle) against M_n.

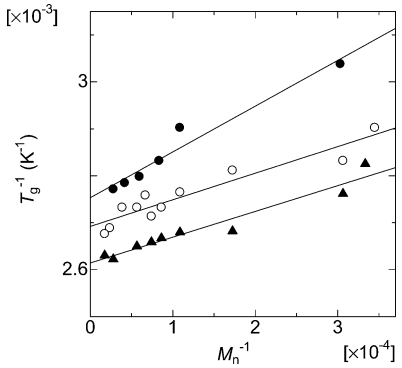

Figure 5. $T_{g,i}^{-1}$ (open), $T_{g,e}^{-1}$ (solid), and $T_{g,DSC}^{-1}$ (triangle) vs M_n^{-1}. Solid lines present eq 1 for all data with $T_{g\infty,i}$ = 374 K, A_i = 0.56, $T_{g\infty,e}$ = 366 K, A_e = 0.98, $T_{g\infty,DSC}$ = 383 K, and A_{DSC} = 0.55.

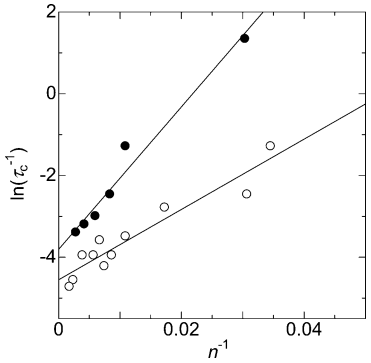

Figure 6. Plots of $\ln(1/\tau_i)$ (open) and $\ln(1/\tau_e)$ (solid) against inverse of n. Data were fitted by the least-squares method. $\ln(1/\tau_i) = 86/n - 4.6$ and $\ln(1/\tau_e) = 174/n - 3.8$.

degradation of the spin-labels. Therefore, the $T_{5.0mT}$ more than 450 K was extrapolated by fitting using an arctangent curve near the transition region. In general, the temperature-dependent extreme separation width around the $T_{5.0mT}$ is fitted well by some arctangent function (e.g., Figure 3 in ref 2 and Figure 4 in ref 3). To examine the accuracy of this extrapolation, the inverse of $T_{5.5mT}$ (temperature at which the extreme separation width is equal to 5.5 mT) of the PMMA was plotted against the $1/M_n$ (figure is not shown), and the plots were fitted by eq 1 as well as Figure 5. $T_{5.5mT,\infty}$'s (the $T_{5.5mT}$ at the infinite M_n) of the PMMA labeled at the inside and the chain end were estimated to be 455 and 447 K, respectively. The difference between these values was 8 K, and this was in good agreement with the $\Delta T_{5.0mT}$ of the PMMA of 8 K (see Figure 7). This means the extrapolation of the $T_{5.0mT}$ provides a good estimation.

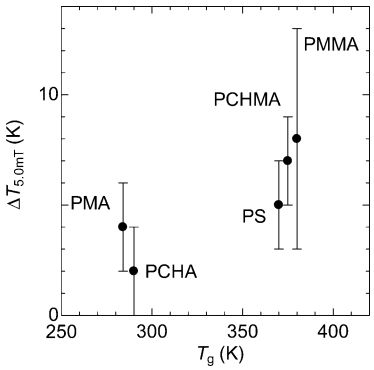

Figure 7. Plots of $\Delta T_{5.0mT}$ against T_g for various polymers.

The $T_{5.0mT}$ appears at higher temperature than the T_g of the PMMA determined by the DSC because of a high frequency corresponding to the rate of averaging of the anisotropic hyperfine splitting.[2,34−36] The difference between the T_g and $T_{5.0mT}$ was discussed in detail in the section below. The high mobility around chain ends was directly detected. The higher mobility around chain ends can be rationalized in the free volume model, the entropy model, and the coupling model by the chain ends having respectively excess free volume, excess configurational entropy, and deficient intermolecular constraints.[7,8]

Recently, Kajiyama and co-workers reported that the T_g in the polymer surface region is lower than that of the bulk.[38−44] They interpreted the depression of the surface T_g in term of the enrichment of end groups and the free space on the surface. In particular, their studies on the segmental diffusion at the interface of the bilayer film made from PS and deuterated PS films revealed the segmental diffusion at the interface below the T_g of the bulk PS.[43,44] In this case, the nature of the free space on the surface is considered to be canceled because of the lamination. Therefore, the depression of the T_g at the interfacial region evidenced that the enriched chain ends at the interface. The lower $T_{5.0mT,e}$ than the $T_{5.0mT,i}$ supports their results.

In polymer solutions, the molecular mobility of chain ends is higher than that of the inside segments because of the lower potential barrier for the configurational transition of the main chain bond of the chain end.[45−47]

Santangelo et al. estimated the molecular weight dependence of the "fragility" of PS,[19] and a decrease in the fragility of the PS with a reduction of the molecular weight was indicated. This behavior was interpreted that an increase in any configurational freedom conferred by chain ends reduced the fragility. Our direct detection of the high mobility around chain ends bolsters their consideration.

2. Molecular Weight Dependence of $T_{5.0mT,i}$ and $T_{5.0mT,e}$. The $T_{g,DSC}$, $T_{5.0mT,i}$, and $T_{5.0mT,e}$ are plotted against the M_n of PMMA in Figure 4. The $T_{g,DSC}$ was taken to be the midpoint, i.e., the temperature corresponding to half of the endothermic shift and included ±1.5 K of experimental errors. All transition temperatures decreased with the reduction of the M_n. Fox and Flory first interpreted that the T_g decreases with the increase in the chain end fraction.[7,48] In other words, the increase in the mobile chain end brings the decrease in the overall T_g. In fact, the $T_{5.0mT,e}$ is lower than the $T_{5.0mT,i}$.

The difference between the T_g and $T_{5.0mT}$ was interpreted with the WLF equation. The WLF equation is the successful relationship of temperature dependence for the viscous flow, viscoelastic response, and dielectric dispersion of polymers and supercooled liquids.[49]

$$\log a_T = -C_{1g}(T - T_0)/[C_{2g} + (T - T_0)] \qquad (2)$$

where a_T is the temperature shift factor that is the ratio of a τ_c at the chosen reference temperature, T_0, to that at the temperature of measurement, T. When T_0 was chosen to be the T_g, constants C_{1g} and C_{2g} for PMMA are 16.15 and 53.4, respectively.[50] The relaxation time of 7×10^{-9} and 100 s are used as the τ_c's of the ESR and DSC, respectively.[51,52] The ΔT ($= T_{5.0mT} - T_{g,DSC}$) are calculated to be 90 K from eq 2. On the other hand, the ΔT ($= T_{5.0mT\infty,i} - T_{g\infty,DSC}$) obtained from the experiments are 81 K, where the $T_{5.0mT\infty,i}$ and $T_{g\infty,DSC}$ are the asymptotic values of the $T_{5.0mT,i}$ and $T_{g,DSC}$ for the infinite molecular weight in Figure 4. Even though the difference of 9 K between the calculated and the experimental values exists, the difference is considered to be within experimental errors. The $T_{5.0mT}$ is considered to reflect the glass transition observed at the higher frequency of the ESR. Note that the spin-label used in this work was connected to a sidegroup although the size of the spin-label was comparable with that of the MMA monomer. According to Ngai et al., chains with more rigid backbones or sterically hindering pendant groups exhibit "fragile" relaxation behavior, while "strong" polymers have smooth, compact, or symmetrical structure.[53] Angell explained that the strong cooperativity is one of the causes of the steep increase in the τ_c of "fragile" glasses below T_g.[15] The rigidity of the PMMA is high, and the cooperativity is considered to be strong.[54] Therefore, the spin-labels might move cooperatively with repeat units of the PMMA.

The $T_{5.0mT,i}$ and $T_{5.0mT,e}$ were reduced to transition temperatures, $T_{g,i}$ and $T_{g,e}$, for $\tau_c = 100$ s by the WLF equation, respectively, and the inverse of the $T_{g,i}$, $T_{g,e}$, and the $T_{g,DSC}$ are plotted against the reciprocal of the M_n (Figure 5).[1] The linear relationship of eq 1 gives $T_{g\infty,i}$ and A_i to be 374 K and 0.56, respectively. Similarly, $T_{g\infty,DSC}$ and A_{DSC} were determined to be 383 K and 0.55, respectively. The A_{DSC} and A_i are in good agreement with each other. This result indicates that the $T_{5.0mT,i}$ is the T_g observed at the high frequency of the ESR, and the molecular weight dependence on the WLF parameters might be able to be ignored for these molecular weights (M_n > ca. 3K).

$T_{g\infty,e}$ and A_e were determined to be 366 K and 0.98, respectively. The difference between $T_{g\infty,i}$ and $T_{g\infty,e}$ of the PMMA (ca. 8 K) is somewhat larger than that of the PS (ca. 5 K) reported previously.[2] Rizos and Ngai considered that the difference in mobility between chain ends and inside segments is expected to be larger for polymers that have greater intermolecular coupling or high "fragility" because greater intermolecular cooperativity results in much lower mobility of the inside segments.[20] The fragility indexes of PMMA and PS were reported to be 145 and 139, respectively.[54] It is considered that the differences in mobility between chain ends and inside segments of PMMA is somewhat larger than that of the PS because the fragility index of PMMA is somewhat larger than that of the PS.

The molecular weight dependence of the $T_{g,e}$ suggests that the $T_{g,e}$ reflected the α relaxation of the PMMA and not the other local motions (β and γ relaxations) because the local motions might have no molecular weight dependence. The molecular weight dependence of the

$T_{g,e}$ indicates the cooperative motion of chain end segments with neighboring inside segments. In other words, the flexibility around chain ends makes the $T_{g,e}$ depressed, but the cooperative motion with neighboring segments is considered to be necessary for not only inside segments but also chain end segments to undergo a rotational relaxation. Therefore, the molecular weight dependence of the $T_{g,e}$ can be interpreted in term of the influence of the neighboring inside segments.

3. Strong M_n Dependence of $T_{5.0mT,e}$. The A_e was roughly twice larger than the A_i. The larger A_e than the A_i indicates the strong molecular weight dependence on the mobility around chain ends; namely, the mobility around chain ends is more enhanced than that of inside segments with the decrease in the molecular weight. This behavior was previously observed for PS.[2] These results are interesting to understand dynamic features of chain ends. In the previous paper, a simple model on the basis of the probability of an encounter of chain ends was suggested to interpret the strong molecular weight dependence of the $T_{g,e}$.[2] As described above, the cooperative motion with neighboring segments is necessary in the bulk. This model bases on an idea that the encounter of chain ends locally increases mobility around them.

In this model, it is assumed that one noticed segment is surrounded with four other segments, and the combination of an arrangement of each segment in this situation is considered. Four surrounding segments consist of four polymeric chains including eight end segments. When the number of the segments in one polymeric chain, n, is large, the probability that the noticed segment is surrounded with four inside segments is calculated to be approximately $1 - 9.5/n$ as mentioned in detail in our previous paper.[2] Similarly, $8/n$ is obtained approximately for the probability that the noticed segment is surrounded with three inside and one end segments. The other probabilities can be ignored because they are relatively too small. When a chain end segment is surrounded with four segments, the average relaxation rate ($1/\tau_e$) of the spin-labels at the chain end could be given as

$$\ln(1/\tau_e) = (1 - 9.5/n)\ln(1/\tau_{e-i_4}) + (8/n)\ln(1/\tau_{e-i_3e_1}) = [8\ln(1/\tau_{e-i_3e_1}) - 9.5\ln(1/\tau_{e-i_4})]/n + \ln(1/\tau_{e-i_4}) \quad (3)$$

Here, τ_{e-i_4} is the relaxation time in the case of the end segment is surrounded with four inside segments. $\tau_{e-i_3e_1}$ expresses the relaxation time that the end segment is surrounded with one end and three inside segments. Similarly, the average relaxation rate of the spin-labels at the inside of the chain ($1/\tau_i$) is expressed by

$$\ln(1/\tau_i) = (1 - 9.5/n)\ln(1/\tau_{i-i_4}) + (8/n)\ln(1/\tau_{i-i_3e_1}) = [8\ln(1/\tau_{i-i_3e_1}) - 9.5\ln(1/\tau_{i-i_4})]/n + \ln(1/\tau_{i-i_4}) \quad (4)$$

The n was first defined as a degree of polymerization to compare the eqs 3 and 4 with experimental results for simplicity. The $\ln(1/\tau_i)$ and $\ln(1/\tau_e)$ determined from the experiment were plotted against the inverse of the n, and the data were fitted with linear relation according to eqs 3 and 4 in Figure 6. Here, the τ_e and τ_i were calculated using the WLF equation with the reference temperature of 374 K with $\tau_c = 100$ s. The intercept terms of the fitted lines give the τ_{i-i_4} and τ_{e-i_4} to be ca. 100 and 40 s, respectively. The shorter τ_{e-i_4} than the τ_{i-i_4} is reasonable because the mobility around chain ends is higher than that of inside segments. When one considers the segment size related to the motion, it is actually inappropriate to use the degree of polymerization as the segmental unit. Thus, a number of motional segments per one PMMA chain, n', is given by $n' = n/x$, where x is the monomeric unit number involved in one motional segment. Then, the n' should be substituted into the n in eqs 3 and 4. When the $\tau_{i-i_3e_1}$ is assumed to be identical with the τ_{e-i_4}, the x is estimated to be 7 from the slope of the fitted line and eq 4.

According to Lodge et al., the cooperative volume above the glass transition is comparable to the l_k^3.[23] Haley et al. reported that the cooperative volume relevant to the dynamics of the components in the blend was nearly temperature-independent above the T_g.[27] Recently, we suggested that the volume relevant to the motion of spin-labels in the PCHMA/PCHA miscible blend agreed with the l_k^3.[28] The l_k^3 of the PMMA is calculated to be ca. 2.6 nm^3.[23] On the other hand, the cooperative volume estimated in this work is ca. 1.0 nm^3.[55] We consider that these values are almost coincident with each other.

When the x around chain ends is assumed to be equal to that of inside segments, the $\tau_{e-i_3e_1}$ is calculated to be ca. 3 s from the slope of the fitted line in Figure 6 and eq 3. The shorter relaxation time $\tau_{e-i_3e_1}$ (= ca. 3 s) than the τ_{e-i_4} (= ca. 40 s) was obtained. The encounter of chain ends induced the much shorter relaxation time around them. This behavior might be explained that the cooperativity between segments was locally weakened by the encounter of chain ends. A decrease in the M_n brings the increase in the chain end fraction, necessarily leading to increasing the probability of the encounter of chain ends. When the motion of chain ends is noticed, the encountering of chain ends cannot be ignored in the case that the concentration of chain ends is high. In fact, as an analogous example, the increased mobility around chain ends was observed for microphase-sepatrated polystyrene-*block*-poly(methyl acrylate) with a lamellar morphology.[3] In this case, the chain ends were concentrated around the center of lamellar domains because of the relatively stretched chain conformation to the perpendicular to the lamellar interface. We insist the idea that the locally enhanced mobility induced by the encounter of chain ends is unable to be ignored on the glass transitions of polymers when the chain end concentration is (locally) high.

4. Relationship between Chain End Effect and Mobility of Main Chain. We determined the difference in mobility between chain ends and inside segments for PMMA, PS, PCHMA, PCHA, and PMA by the spin-label techniques.[2–4] The difference between the $T_{5.0mT,i}$ and $T_{5.0mT,e}$, $\Delta T_{5.0mT}$'s, of the polymers were plotted against their T_g's (Figure 7). The $\Delta T_{5.0mT}$ increased with an increase in the T_g. Note that the M_n's of the PCHMA, PCHA, and PMA are 12K, 15K, and 30K, respectively. Here, the each $\Delta T_{5.0mT}$ of these polymers is M_n-dependent at least as for the PS and PMMA. Therefore, the $\Delta T_{5.0mT}$'s of these polymers at the infinite M_n should be somewhat smaller than those plotted in Figure 7.

Santangelo et al. reported that the fragility of PS decreased with the reduction of the M_n.[19] They concluded that any conformational freedom conferred from chain ends reduced the fragility. On the other hand, the

fragility of poly(dimethylsiloxiane) (PDMS) was nearly M_n-independent because the ether linkage in the PDMS backbone gave nearly free rotation.[56] From these results, Rizos and Ngai pointed out that the difference in mobility between chain ends and inside segments is expected to be larger for polymers that have greater intermolecular coupling or large "fragility" because greater intermolecular cooperativity results in much lower mobility of the inside segments.[20] In fact, the T_g of high-T_g polymers is generally more sensitive to the molecular weight (or the chain end fraction).[57,58] These results imply that the difference in mobility between chain ends and inside segments is large for high-T_g polymers, and the chain end effect on the dynamics is more remarkable. It seems that the result in Figure 7 agrees well with these reports. However, this spin-label technique essentially detects motion of nitroxides (spin-labels). Therefore, one has to consider the difference in the interaction between nitroxides and host polymers to estimate the result in Figure 7. We consider that further experiments are required to insist strongly the result in Figure 7. Estimation of mobility around chain ends by nonlabel techniques is expected.

Conclusion

The high molecular mobility around chain ends of PMMA was directly detected by the spin-label technique. The $T_{g\infty,e}$ was ca. 8 K lower than the $T_{g\infty,i}$ because of the flexibility around chain ends. The trend of that the $\Delta T_{5.0mT}$ decreased with the reduction of the T_g of polymers because of the high mobility of inside segments of the low-T_g polymers was shown. The molecular weight dependence of the $T_{g,e}$ implied the cooperative motion of chain end segments with neighboring inside segments. The size of the cooperative volume was estimated to be ca. 1 nm^3 by the model on the basis of the arrangement of segments. This value was almost coincident with the l_k^3 (=2.6 nm^3) which is the cooperative volume proposed by Lodge et al. Our model suggested that the encounter of chain ends locally induced shorter τ_c around them. In conclusion, chain ends have higher mobility and the encounter of chain ends cannot be ignored on the mobility of chain ends in the case of high concentration of chain, that is, in the case of a low molecular weight.

Acknowledgment. This research was partially supported by the Ministry of Education, Science, Sports and Culture, Grant-in-Aid for Young Scientists (B), 16750185, 2004 and the NITECH 21st Century COE Program "World Ceramics Center for Environmental Harmony". Thanks are due to the Research Center for Molecular-Scale Nanoscience, the Institute for Molecular Science, for assistance in obtaining the DSC and the MALDI-TOF-MS data.

References and Notes

(1) Ueberreiter, K.; Kanig, G. *J. Colloid Sci.* **1952**, *7*, 569.
(2) Miwa, Y.; Tanase, T.; Yamamoto, K.; Sakaguchi, M.; Sakai, M.; Shimada, S. *Macromolecules* **2003**, *36*, 3235.
(3) Miwa, Y.; Yamamoto, K.; Sakaguchi, M.; Sakai, M.; Tanida, K.; Hara, S.; Okamoto, S.; Shimada, S. *Macromolecules* **2004**, *37*, 831.
(4) Miwa, Y.; Tanabe, T.; Yamamoto, K.; Sugino, Y.; Sakaguchi, M.; Sakai, M.; Shimada, S. *Macromolecules* **2004**, *37*, 8612.
(5) Faller, R. *Macromolecules* **2004**, *37*, 1095.
(6) Tokita, N.; Hirabayashi, M.; Azuma, C.; Dotera, T. *J. Chem. Phys.* **2004**, *120*, 496.
(7) Fox, T. G.; Flory, P. J. *J. Polym. Sci.* **1954**, *14*, 315.
(8) Ngai, K. L.; Plazek, D. J.; Echeverria, I. *Macromolecules* **1997**, *29*, 77937.
(9) Yu, W.; Sung, C. S. P.; Robertson, R. E. *Macromolecules* **1988**, *21*, 355.
(10) Yu, W.; Sung, C. S. P. *Macromolecules* **1988**, *21*, 365.
(11) Li, H.; Ujihira, Y.; Nanasawa, A. *Kobunshi Ronbunshu* **1996**, *53*, 358.
(12) Richardson, M. J.; Savill, N. G. *Polymer* **1977**, *18*, 3.
(13) Kanaya, T.; Tsukushi, T.; Kaji, K.; Bartos, J.; Kristiak, J. *Phys. Rev.* **1999**, *60*, 1906.
(14) Bartoš, J.; Bandžuch, P.; Šauša, O.; Krištiaková, K.; Krištiak, J.; Kanaya, T.; Jenninger, W. *Macromolecules* **1997**, *30*, 6906.
(15) Angell, C. A. *J. Phys. Chem. Solids* **1988**, *49*, 863.
(16) Angell, C. A. *J. Non-Cryst. Solids* **1991**, *131*−*133*, 13.
(17) Angell, C. A. *Science* **1995**, *267*, 1924.
(18) Angell, C. A.; Poole, P. H.; Shao, J. *Nuovo Cimento* **1994**, *16*, 883.
(19) Santangelo, P. G.; Roland, C. M. *Macromolecules* **1998**, *31*, 4581.
(20) Rizos, A. K.; Ngai, K. L. *Macromolecular* **1998**, *31*, 6217.
(21) Casalini, R.; Santangelo, P. G.; Roland, C. M. *J. Phys. Chem. B* **2002**, *106*, 11492.
(22) Inoue, T.; Osaki, K. *Macromolecules* **1996**, *29*, 1595.
(23) Lodge, T. P.; McLeish, T. C. *Macromolecules* **2000**, *33*, 5278.
(24) Kant, R.; Kumar, S. K.; Colby, R. *Macromolecules* **2003**, *36*, 10087.
(25) Leroy, E.; Alegría, A.; Colmenero, J. *Macromolecules* **2002**, *35*, 5587.
(26) Leroy, E.; Alegría, A.; Colmenero, J. *Macromolecules* **2003**, *36*, 7280.
(27) Haley, C. J.; Lodge, P. T.; He, Y.; Ediger, M. D.; von Meerwall, E. D.; Mijovic, J. *Macromolecules* **2003**, *36*, 6142.
(28) Miwa, Y.; Sugino, Y.; Yamamoto, K.; Tanabe, T.; Sakaguchi, M.; Sakai, M.; Shimada, S. *Macromolecules* **2004**, *37*, 6061.
(29) Matyjaszewski, K.; Shipp, D. A.; Wang, J. L.; Grimaud, T.; Patten, T. E. *Macromolecules* **1998**, *31*, 6836.
(30) Xia, J.; Matyjaszewski, K. *Macromolecules* **1997**, *30*, 7697.
(31) Ziegler, M.; Matyjaszewski, K. *Macromolecules* **2001**, *34*, 415.
(32) Nonaka, H.; Ouchi, M.; Kamigaito, M.; Sawamoto, M. *Macromolecules* **2001**, *34*, 2083.
(33) Cho, D.; Park, S.; Kwon, K.; Chang, T.; Roovers, J. *Macromolecules* **2001**, *34*, 7570.
(34) Shimada, S.; Kashima, K. *Polym. J.* **1996**, *28*, 690.
(35) Sohma, J.; Sakaguchi, M. *Adv. Polym. Sci.* **1978**, *20*, 109.
(36) Kusumoto, N.; Sano, S.; Zaitsu, N.; Motozato, Y. *Polymer* **1976**, *17*, 448.
(37) Schlick, S.; Harvey, R. D.; Alonso-Amigo, M. G.; Klempner, D. *Macromolecules* **1989**, *22*, 822.
(38) Tanaka, K.; Taura, K.; Takahara, A.; Kajiyama, T. *Macromolecules* **1996**, *29*, 3040.
(39) Kajiyama, T.; Tanaka, K.; Takahara, A. *Macromolecules* **1997**, *30*, 280.
(40) Tanaka, K.; Jiang, X.; Nakamura, K.; Takahara, A.; Kajiyama, T.; Ishizoe, T.; Hirao, A.; Nakahama, S. *Macromolecules* **1998**, *31*, 5148.
(41) Xie, F.; Zhang, H. F.; Lee, F. K.; Du, B.; Tsui, O. K. C.; Yokoe, Y.; Tanaka, K.; Takahara, A.; Kajiyama, T.; He, T. *Macromolecules* **2002**, *35*, 1491.
(42) Tanaka, K.; Takahara, A.; Kajiyama, T. *Macromolecules* **2000**, *33*, 7588.
(43) Kawaguchi, D.; Tanaka, K.; Takahara, A.; Kajiyama, T. *Macromolecules* **2001**, *34*, 6164.
(44) Kawaguchi, D.; Tanaka, K.; Kajiyama, T.; Takahara, A.; Tasaki, S. *Macromolecules* **2001**, *34*, 6164.
(45) Waldow, D. A.; Ediger, M. D.; Yamaguchi, Y.; Matsushita, Y.; Noda, I. *Macromolecules* **1991**, *24*, 3147.
(46) Adolf, D. B.; Ediger, M. D.; Kitano, T.; Ito, K. *Macromolecules* **1992**, *25*, 867.
(47) Horinaka, J.; Maruta, M.; Ito, S.; Yamamoto, M. *Macromolecules* **1999**, *32*, 1134.
(48) Fox, T. G.; Flory, P. J. *J. Appl. Phys.* **1950**, *21*, 581.
(49) Williams, M. L.; Landel, R. F.; Ferry, J. D. *J. Am. Chem. Soc.* **1995**, *77*, 3701.
(50) Plazek, D. J.; Ngai, K. L. *Macromolecules* **1991**, *24*, 1222.
(51) Törmälä, P.; Weber, G. *Polymer* **1978**, *19*, 1026.
(52) Ngai, K. L.; Plazek, D. J. *Rubber Chem. Tecnol.* **1995**, *68*, 376.
(53) Ngai, K. L.; Roland, C. M. *Macromolecules* **1993**, *26*, 6824.

(54) Böhmer, R.; Ngai, K. L.; Angell, C. A.; Plazek, D. J. *J. Chem. Phys.* **1993**, *99*, 4201.
(55) The cooperative volume of the PMMA was calculated from $7V_m$. V_m is the volume of a MMA monomeric unit, and it was estimated to be ca. 140 Å^3. (Tsay, F. D.; Gupta, A. *J. Polym. Sci., Part B: Polym. Phys.* **1987**, *25*, 855).
(56) Roland, C. M.; Nagai, K. L. *Macromolecules* **1996**, *29*, 5747.
(57) Boyer, R. F. *Macromolecules* **1974**, *7*, 142.
(58) Cowie, J. M. G. *Eur. Polym. J.* **1975**, *11*, 297.

MA048287Y